

EUROPHYSICS LETTERS

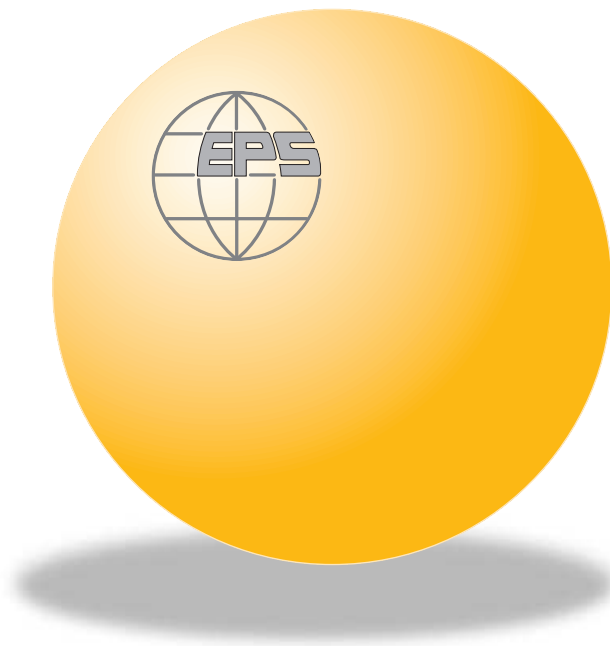
OFFPRINT

Vol. 66 • Number 6 • pp. 798–804

**Acoustic second-harmonic generation with shear
to longitudinal mode conversion in granular media**

* * *

V. TOURNAT, V. E. GUSEV, V. YU. ZAITSEV and B. CASTAGNÈDE



Published under the scientific responsibility of the
EUROPEAN PHYSICAL SOCIETY
Incorporating
JOURNAL DE PHYSIQUE LETTRES • LETTERE AL NUOVO CIMENTO

Acoustic second-harmonic generation with shear to longitudinal mode conversion in granular media

V. TOURNAT¹, V. E. GUSEV¹, V. YU. ZAITSEV² and B. CASTAGNÈDE¹

¹ *Université du Maine - Av. Olivier Messiaen, 72085 Le Mans Cedex 9, France*

² *Institute of Applied Physics - 46 Uljanova Street, Nizhny Novgorod, 603950 Russia*

(received 20 August 2003; accepted in final form 15 April 2004)

PACS. 43.25.+y – Nonlinear acoustics.

PACS. 83.80.Fg – Granular solids.

PACS. 81.05.Rm – Porous materials; granular materials.

Abstract. – Excitation of longitudinal acoustic wave at the 2nd harmonic by sinusoidal shear acoustic wave in a granular material is reported. The amplitude of the 2nd harmonic exhibits beatings (typical of nonlinear processes in dispersive media), which are observed not as a function of the distance from emitter, but with increasing amplitude of the primary (pump) shear wave. The effect is attributed to varying contribution of clapping intergrain contacts to the total nonlinearity of the medium with increasing pump amplitude, which modifies the effective length of the nonlinear interaction. This is consistent with the idea that in granular assemblages there is an important amount of contacts loaded much weaker than in average.

Introduction. – Second-harmonic excitation is a classical nonlinear effect which is useful, for example, for frequency up-conversion in optics [1,2] and material characterization in acoustics [3–5]. The efficiency of the transformation of the pump wave at fundamental frequency ω into its 2nd harmonic at frequency 2ω is determined not only by the local nonlinearity of a medium, but also depends on the possibility to synchronously accumulate locally excited 2ω -waves. The synchronism conditions are closely related to the wave velocity dispersion in the medium. In the case of collinear wave interaction, the nonlinear sources at 2ω (produced by the pump wave) propagate with the phase velocity of the pump wave $c(\omega) = \omega/k(\omega)$, while the excited second harmonic propagates with velocity $c(2\omega) = 2\omega/k(2\omega)$. Here k denotes the wave number. If $c(\omega) \neq c(2\omega)$ (*i.e.* $\Delta k \equiv k(2\omega) - 2k(\omega) \neq 0$), the beating of the forced and free waves occurs. Such beating is a hallmark of dispersive nonlinear interactions [1, 2, 6, 7]. This leads to periodic spatial modulation of the 2ω amplitude along the interaction length, and the beating spatial period limits the accumulation (coherence) length of the second harmonic by $L_c = \pi/\Delta k$. In optics, where the attenuation of the pump wave is negligible, the length of the nonlinear crystal should be optimized correspondingly.

In acoustics, the dispersion is usually much less than in optics, and the 2ω excitation in a homogeneous medium is quasi-synchronous with 2ω -wave accumulation limited by the pump wave absorption or diffraction. Dispersion is characteristic of acoustic modes in waveguides, where the periodic spatial modulation of sum- and difference-frequency sound amplitude was

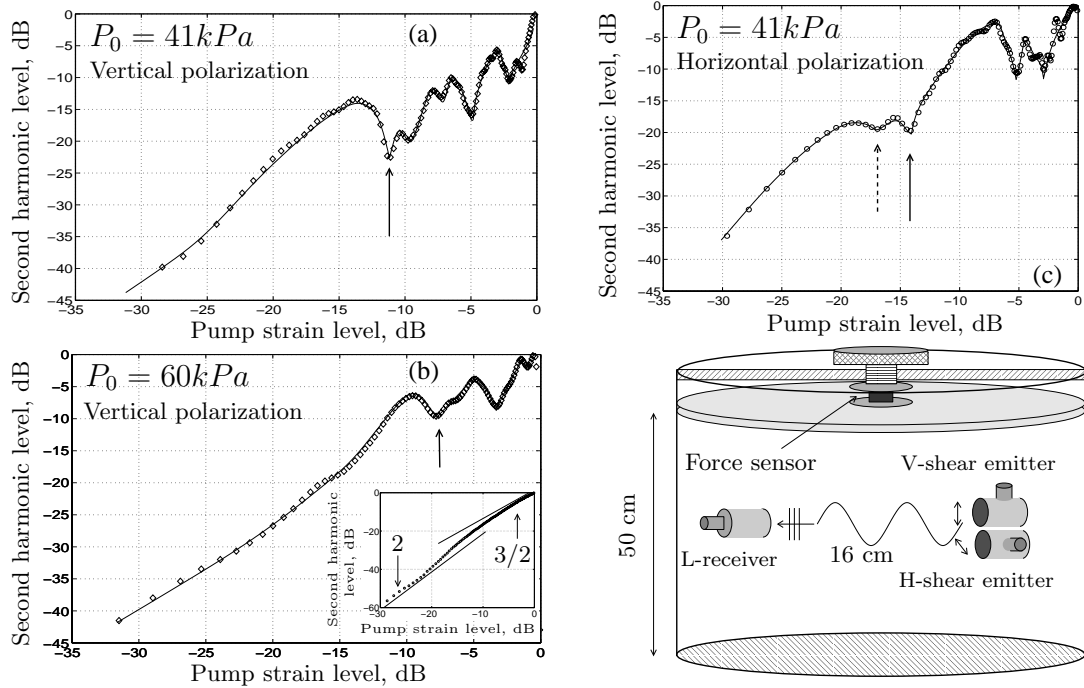


Fig. 1 – Scheme of the experiment and longitudinal second-harmonic level as a function of the shear pump strain level. Vertically polarized pump (V-shear), plots (a) and (b). Horizontally polarized pump (H-shear), plot (c). Insert in plot (b) is for the longitudinal pump.

experimentally observed [6]. A similar effect was reported for Rayleigh surface waves for which the dispersion was introduced by loading the substrate with a thin film [7, 8]. It was demonstrated experimentally that dispersion suppresses higher-harmonics generation in surface acoustic waves [9].

In the present letter we describe observations of beatings in the amplitude of the second harmonic excited in a granular medium. There are two important differences between the references cited above and our experiments.

First, the asynchronism between the nonlinear force and the second-harmonic wave in our experiments is not due to velocity dispersion for a single acoustic mode, but due to the mode conversion in the nonlinear process. It is well known that the excitation of the longitudinal (L) acoustic wave at 2ω by the shear (S) acoustic pump wave at ω is theoretically allowed in solids [3]. However, to the best of our knowledge, this process has never been experimentally observed because of the weak nonlinearity of homogeneous solids and the large difference between the velocities c_L and c_S of L- and S-waves [3]. The first of these two factors (limiting 2ω -wave amplitude) was overcome in our experiment by choosing the granular material in which the nonlinear parameter exceeds those typical of homogeneous solids by two to four orders in magnitude (depending on the level of external static pre-loading) [10, 11].

Second, the beatings in the 2ω amplitude are found not when the observation distance is varying, but when the amplitude of the pump S-wave is increased. Theoretical estimates presented below attribute this effect to the nonlinear transformation of the wave interaction region, caused by the change in the mechanism of the 2ω excitation with the increasing pump amplitude.

Experiment. – The scheme of the experiment is shown in fig. 1. The emitter excited S-waves at frequency $f = 5.12$ kHz with vertical (V) or horizontal (H) polarization and the estimated S-wave length $\lambda_\omega \simeq 4.4$ cm, the observation distance being $R \simeq 16$ cm (see fig. 1) (the chosen 5–10 kHz frequency range allowed for quasi-free field propagation and provided negligible scattering by the structural disorder). For the transducer of radius $a \simeq 2$ cm, the diffraction length $L_d \sim \pi a^2/\lambda_\omega \sim 3$ cm is comparable to the transducer dimensions, so that the excitation of the 2ω -signal takes place in the essentially spherically diverging geometry. Variation of the external stress by an order of magnitude $7.2 \text{ kPa} \leq P_0 \leq 72 \text{ kPa}$ changed the average static strain from $\varepsilon_0 \simeq 7 \cdot 10^{-5}$ to $\varepsilon_0 \simeq 3.3 \cdot 10^{-4}$ (here the compression corresponds to positive strain). The glass beads were of 2 mm diameter. The receiver was created for the L-polarization, so that its residual sensitivity to S-polarized waves was significantly reduced. It was verified that the received signal at 2ω corresponded to the L-wave, for which the signal delay and polarization were checked. The observed S to L nonlinear mode conversion is allowed by the symmetry considerations, whereas conversion of S to 2ω S-wave in isotropic homogeneous materials is forbidden [3].

In fig. 1 parts (a) and (b), the dependence of the 2ω amplitude on the amplitude of the V-polarized S-pump is presented. The beatings are clearly visible and reproducible. On the x -axis, 0 dB corresponds to the maximal used pump strain amplitude about $\tilde{\varepsilon}_a^{\text{max}} \simeq 1.4 \cdot 10^{-5}$. It is more than an order of magnitude less than the average static strains in the medium ($2.3 \cdot 10^{-4}$ and $2.9 \cdot 10^{-4}$ for the applied static stresses 41 kPa and 60 kPa, respectively). Thus on the x -axis the average static strain of the medium is located around ~ 20 dB and higher. In fig. 1(b), the measurements correspond to a larger static preloading than in fig. 1(a). Comparison of the figures indicates the shift of the first local minimum (marked by vertical arrows) to higher pump amplitude for higher static strain.

In fig. 1(c), the dependence of the L-amplitude at 2ω on the amplitude of the H-polarized S-pump is shown for the same static loading as in the case of V-polarization in fig. 1(a). Comparison of the figures demonstrates that the first minimum appears for the H-polarized pump at smaller amplitudes than for the V-polarized one.

The main observed features were found to be qualitatively reproducible if the granular medium had been prepared following this procedure: a) filling the container with the beads, b) tapping without static load, c) application of a slowly increasing static load, d) strong acoustic excitation (at different frequencies). However, slight changes in the minima positions were observed even at superimposing different acquisitions in the same configuration, and were attributed to slow dynamic effects which are beyond the scope of the present letter.

Discussion. – We attribute the beating in the 2nd-harmonic amplitude to the unproportional modification of the spatial distribution of the nonlinear 2ω sources with increasing pump amplitude. Nonlinear acoustic experiments in granular media indicate that, at sufficiently strong excitation, the weak clapping inter-grain contacts can provide competitive [12, 13] or even dominant [11] contribution to the nonlinear part of the stress-strain relation $\sigma(\varepsilon)$ if compared with the contribution from contacts which remain closed during the whole period of acoustic loading. Indeed, in real granular materials, a significant portion of contacts is loaded much weaker than in average [11, 12], which essentially contributes to the resultant nonlinearity of $\sigma(\varepsilon)$. Let us model, for simplicity, the distribution of weak contacts by a single fraction statically pre-loaded by the strain $\mu\varepsilon_0$ (which for $\mu \ll 1$ is significantly lower than the average loading ε_0). Separating out the static (σ_0, ε_0) and oscillatory ($\tilde{\sigma}, \tilde{\varepsilon}$) contributions, the stress-strain relation may be rewritten as

$$\sigma_0 + \tilde{\sigma} = bn_0(\varepsilon_0 + \tilde{\varepsilon})^{3/2}H(\varepsilon_0 + \tilde{\varepsilon}) + bn_1(\mu\varepsilon_0 + \tilde{\varepsilon})^{3/2}H(\mu\varepsilon_0 + \tilde{\varepsilon}). \quad (1)$$

Here $H(\dots)$ is the Heaviside function; n_0 and n_1 are the mean numbers of average-loaded and weak contacts per grain, and factor b depends on elastic moduli of grains and the porosity of the packing. Estimates based on wave velocities data in grainy materials indicate that $n_{0,1}$ may be comparable ($n_0 \sim n_1$) [13]. The nondimensional coefficient $|\mu| \ll 1$ characterizes the extent of unloading of the softer fraction. The power $3/2$ in eq. (1) corresponds to the classical Hertzian nonlinearity. Below, we consider only positive $0 < \mu \ll 1$ corresponding to initially weakly compressed contacts. Then for $|\tilde{\varepsilon}| \ll \mu\varepsilon_0$, the first and higher derivatives of eq. (1) with respect to $\tilde{\varepsilon}$ characterize the linear and nonlinear elastic moduli of the material, respectively:

$$\frac{\partial^m \tilde{\sigma}(\varepsilon_0)}{\partial \tilde{\varepsilon}^m} \sim bn_0 \left(1 + \frac{n_1}{n_0} \mu^{3/2-m} \right) \varepsilon_0^{3/2-m}. \quad (2)$$

Thus, for the linear modulus ($m = 1$) the relative contribution of the weak contacts is $\sim \mu^{1/2} \ll 1$ and may be negligible. In contrast, for the quadratic ($m = 2$) nonlinear modulus responsible for 2ω excitation, the contribution of the weak fraction is $\sim \mu^{-1/2} \gg 1$ and thus may strongly dominate over the nonlinearity of the average-loaded contacts.

For a propagating wave beam the aforementioned material nonlinearity results in the creation of running virtual nonlinear sources which radiate higher harmonics $n\omega$ or combination frequencies of the pump spectrum. In underwater acoustics, this effect is known as parametric sound radiation, and is mostly used for the frequency down-conversion via difference-frequency $\omega_1 - \omega_2$ generation ($|\omega_1 - \omega_2| \ll \omega_1, \omega_2$, when $\omega_1 \sim \omega_2$). In liquids, where S-waves do not propagate and the nonlinearity is near-perfectly quadratic in the acoustic strain, the effect allows for a relatively simple, but rigorous description. Using the perturbation approach, the stress in the nonlinearly radiated wave may be expressed in the integral form:

$$\sigma^{\text{nl}}(\vec{r}) = \Re e \frac{1}{4\pi} \int Q(\vec{r}') \frac{e^{ik_{\text{rad}}|\vec{r}-\vec{r}'|}}{|\vec{r}-\vec{r}'|} d^3r', \quad (3)$$

where the integration is performed over the volume of the nonlinear sources $Q(\vec{r}') \equiv Q(x', y', z')$ created by the primary (pump) beam; \vec{r} is the position of the observation point, k_{rad} is the wave number of the nonlinearly radiated signal. For liquids, the nonlinear source Q is proportional to the square of the primary wave amplitude: $Q \sim [\tilde{\varepsilon}_a e^{-i\omega t + ikr'}]^2$. In liquids both the primary and the nonlinearly radiated waves are of L-type, dispersion is normally absent and the nonlinear interaction is synchronous. This formally means that the oscillating exponential factors in the nonlinear source and in the radiated wave can perfectly compensate each other.

For the experiments in granular solids, the situation is more complex because of the nonlinear conversion between L- and S-waves. However, for a qualitative description of the observed beating effect we may omit the details of coupling between S- and L-modes (having different polarizations) and will focus on the phase synchronism between the running nonlinear sources and the radiated wave. Integral solution (3) is sufficient for our purpose to discuss the phase properties of the integrand and its functional amplitude behavior in order to explain the beating effect. Concerning the absolute level of the radiated harmonic, certainly the polarization coupling between S- and L-modes may additionally affect the numeric factors compared with those in solution (3).

In the considered case, the nonlinear sources at the 2nd harmonic propagate with the phase velocity of the S-wave: $Q \sim e^{-i2\omega t + i2k_S(\omega)r'}$, where the wave number $k_S = \omega/c_S(\omega)$. The radiated 2nd harmonic of the L-wave propagates with another phase velocity c_L and wave number $k_{\text{rad}} = k_L(2\omega) = 2\omega/c_L(2\omega)$. The oscillating factors of the source and the radiated harmonic thus do not compensate each other and produce beating $\sim e^{i\Delta k r'} = e^{i[k_L(2\omega) - 2k_S(\omega)]r'}$ under

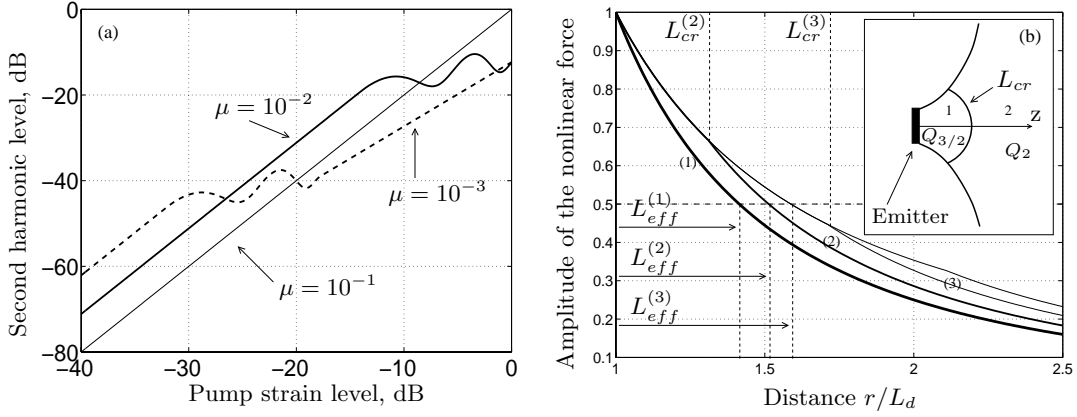


Fig. 2 – Elucidation of the beating effect. (a) 2nd-harmonic calculated using eq. (5) as a function of the S-pump amplitude for three values of the parameter μ . (b) Spatial antenna body transformation for three increased pump levels: $\tilde{\varepsilon}_a(0)/\tilde{\varepsilon}_a^{cr} = 1$, $\tilde{\varepsilon}_a(0)/\tilde{\varepsilon}_a^{cr} = 1.3$, $\tilde{\varepsilon}_a(0)/\tilde{\varepsilon}_a^{cr} = 1.7$ for curves (1)-(3). The respective increased lengths of the antenna at the level $1/2$ are marked as $L_{eff}^{(1)-(3)}$. In the inset the “clapping” and the quadratic regions of the antenna body are qualitatively sketched.

the integral. The half spatial period of the beatings limits the distance over which the contributions of the nonlinear sources are synchronously accumulated. Another important feature of the granular material is that the nonlinear source remains quadratic only for small enough amplitudes $\tilde{\varepsilon}_a$ of the pump strain, $\tilde{\varepsilon}_a/\varepsilon_0 \ll \mu$. In this case, the expansion for eq. (1) leads to the nonlinear source of the form $Q = Q_2 \sim (3/16)(\mu\varepsilon_0)^{-1/2}\tilde{\varepsilon}_a^2$. For stronger $\tilde{\varepsilon}_a > \mu\varepsilon_0$ the nonlinearity is progressively becoming of the clapping type (see the Heaviside function in eq. (1)). Thus, after singling out the 2ω harmonic, the nonlinear source corresponding to the essentially clapping regime of the weak contacts takes the form: $Q = Q_{3/2} \sim (3/4\pi)\tilde{\varepsilon}_a^{3/2}$. The magnitudes of the nonlinear source in the two regimes coincide at $\tilde{\varepsilon}_a^{cr} \simeq 16\mu\varepsilon_0/\pi^2$, which we shall consider as the characteristic transition amplitude between the quadratic and clapping regimes. In this approximation, the interaction region in eq. (3) is subdivided into two parts corresponding to the quadratic/clapping regions of the nonlinear sources:

$$\tilde{\varepsilon}_a^{2\omega}(\vec{r}) \simeq \Re e \frac{\text{const}}{4\pi} \left\{ \int_{r' < L_{cr}} Q_{3/2}(r') \frac{e^{ik_{rad}|\vec{r}-\vec{r}'|}}{|\vec{r}-\vec{r}'|} d^3r' + \int_{r' > L_{cr}} Q_2(r') \frac{e^{ik_{rad}|\vec{r}-\vec{r}'|}}{|\vec{r}-\vec{r}'|} d^3r' \right\}. \quad (4)$$

Schematically, these regions are shown in the inset in fig. 2. At small-amplitude excitation, the clapping region does not exist at all. With increase of the pump amplitude, the clapping region appears near the radiator and extends in the bulk, the transition distance L_{cr} being determined by condition $\tilde{\varepsilon}_a(r = L_{cr}) = 16\mu\varepsilon_0/\pi^2$. The pump wave (see the previous section) is spherically diverging, so that $\tilde{\varepsilon}_a(r) \simeq \tilde{\varepsilon}_a(r = L_d)L_d/r$. Note that $\tilde{\varepsilon}_a(r = L_d)$ is approximately equal to the pump wave amplitude at the radiator $\tilde{\varepsilon}_a(0)$. Performing the integration across the pump beam and approximating $|\vec{r}-\vec{r}'| \simeq r$ in the denominators in eq. (4), the latter is reduced to

$$\tilde{\varepsilon}_a^{2\omega}(R) \simeq \text{const} \Re e \left\{ \frac{\tilde{\varepsilon}_a^{3/2}(0)}{\pi\sqrt{L_d}} \int_{L_d}^{L_{cr}} \frac{e^{i\Delta kz'}}{(z')^{1/2}} dz' + \frac{\tilde{\varepsilon}_a^2(0)}{4(\mu\varepsilon_0)^{1/2}} \int_{L_{cr}}^R \frac{e^{i\Delta kz'}}{z'} dz' \right\}, \quad (5)$$

where $L_{cr} = \pi^2 L_d \tilde{\varepsilon}_a(0)/(16\mu\varepsilon_0)$. Integral (5) is readily expressed via the Fresnel, sine and

cosine integrals. In fig. 2, expression (5) is plotted for three values of the unloading parameter μ and other parameters close to those in the experiment (observation length $R = 16$ cm, $\Delta k = 95 \text{ m}^{-1}$ corresponding to pump at 5.12 kHz, and $c_S = 225 \text{ m/s}$, $c_L = 335 \text{ m/s}$). The pump strain maximum $\tilde{\varepsilon}_a^{\text{max}}(0)$ (0 dB) is chosen an order of magnitude smaller than the static pre-strain ε_0 . The resultant behavior of the harmonic in fig. 2 essentially depends on μ . For example, for $\mu = 10^{-2}$ (in fig. 2) the initially quadratic and then oscillating dependence for the 2nd harmonic is qualitatively similar to the experimental curves shown in fig. 1 for the same pump amplitude range.

It should be mentioned here that our numerical modeling of granular systems with continuous (rather than δ -localized) distribution of contact strain indicated that the necessary condition for the observation of the considered nonlinear acoustic phenomena is the existence of a well-defined (localized in the acoustic strain amplitude) transition from the regime $Q \sim \tilde{\varepsilon}_a^2$ to the regime $Q \sim \tilde{\varepsilon}_a^{3/2}$. It is this well-defined boundary in the smooth distribution of weak contacts (but not real δ -localization), which is an important condition and to which threshold corresponds. These arguments explain why the simplest modeling of the distribution accepted here as a useful guide for qualitative interpretation can serve also for rather precise quantitative estimates.

Physically, the beatings in integral (5) may be understood as follows. In the granular medium, the nonlinear force grows as $\tilde{\varepsilon}_a^2$ everywhere in space unless $\tilde{\varepsilon}_a$ near the emitting transducer exceeds $\tilde{\varepsilon}_a^{\text{cr}}$ (so that $L_{\text{cr}} > L_d$) giving rise to the “clapping” nonlinear force $\sim \tilde{\varepsilon}_a^{3/2}$ (1st integral in eq. (5)). The quadratic sources $\sim \tilde{\varepsilon}_a^2$ (2nd integral in eq. (5)) will persist outside of this region. This unproportional growth of the two regions is equivalent to the variation of the effective length L_{eff} of the nonlinear antenna emitting 2ω . Figure 2 illustrates the distribution of the normalized nonlinear force for different ratios of $\tilde{\varepsilon}_a(0)/\tilde{\varepsilon}_a^{\text{cr}}$. Clearly, there is an increase in the effective length of the antenna with increasing pump amplitude $L_{\text{eff}}^{(1)} < L_{\text{eff}}^{(2)} < L_{\text{eff}}^{(3)}$. The amplitude-dependent variation of L_{eff} is equivalent here to the variation of the length of the frequency-doubling crystal in nonlinear optics. Due to asynchronism between the radiated 2ω L-wave and the running sources created by S-waves the variation of L_{eff} leads to beatings in the received 2ω signal.

The distance Δz between neighboring positions of L_{eff} corresponding to the successive extrema of the harmonic can be roughly estimated from the phasing condition $\Delta z \sim \pi/\Delta k \sim 3.3$ cm. This means that, when the position L_{cr} of the clapping boundary gradually moves through the whole interaction length (following the increase in the pump amplitude), then, for the observation distance $R \sim 16$ cm, there could be not more than $\sim R/\Delta z \sim 4$ -5 intermediate extrema. Further increase in the pump amplitude does not produce additional extrema, but should lead to the appearance of the smooth dependence with slope 3/2, which indicates that the nonlinear sources are in the essentially clapping regime over the whole interaction length. In fig. 2, the plot for $\mu = 10^{-3}$ demonstrates such a curve with completely developed beatings and slopes 2 and 3/2 before and after this region. When the parameter μ is too large (insignificant unloading), the beatings may not appear at all for the amplitudes used (see fig. 2, curve $\mu = 10^{-1}$ with the quadratic slope over the whole amplitude range). This demonstrates the crucial role of weak inter-grain contacts for the nonlinear beatings. Thus, the generation of L-type 2ω harmonic by S-waves provides a sensitive tool for the evaluation of the weak inter-grain forces. The estimate $\mu \sim 10^{-2}$ based on the 2ω -signal observations, correlates well with values inferred from complementary experiments on the high-frequency pump demodulation in granular media [11]. Similarly to ref. [11], the results presented in this letter are consistent with the recent 3D molecular-dynamics simulation [14] of monodisperse unloaded packing with friction indicating an abrupt upturn in distribution of forces at very small values of

force ($\mu^{2/3} < 0.1$), rather than with a smooth law of force distribution predicted both for 2D monodisperse systems with friction [15] and 2D polydisperse frictionless systems [16].

The experimental observations that pump amplitude corresponding to the first minimum increases with external loading and is higher for the V-polarized S-pump than for the H-polarized one are consistent with the ideas that increased loading makes it more difficult to initiate contact clapping ($\tilde{\varepsilon}_a^{\text{cr}}$ grows because ε_0 increases) and that, due to preferential direction of loading (forced chains [17]), the value $\tilde{\varepsilon}_a^{\text{cr}}$ is larger for vertically oriented contacts than for the horizontal ones because ε_0 is larger for the former. The latter statement means that vertical loading induces, in granular packings, anisotropy in the nonlinearity, manifestations of which depend on the direction of particle displacement in the acoustic wave.

Conclusion. – Experimentally observed beatings in the longitudinal 2nd-harmonic amplitude with increase of the S-pump level are attributed to the asynchronous character of the process of 2ω excitation and to the pump-induced variation of the 2ω effective excitation length. The variation of the effective length of the emitting antenna is explained by increasing contribution of the clapping contacts to the nonlinear process.

* * *

This work is supported by a DGA contract No. 00.34.026.00.470.75.65. and Russian Science Support Foundation and RFBR grant No. 02-02-16237 (VZ).

REFERENCES

- [1] LAUTERBORN W., KURZ T. and WIESENFELDT M., *Coherent Optics, Fundamental and Applications* (Springer, Berlin) 1993.
- [2] SANTER E. G., *Nonlinear Optics* (John Wiley & Sons, New York) 1996.
- [3] ZAREMBO L. K. and KRASILNIKOV V. A., *Sov. Phys. Usp.*, **13** (1971) 778.
- [4] YOST W. T. and CANTRELL J. H., in *Rev. Prog. QNDE*, edited by THOMPSON D. O. and CHIMENTI D. E., Vol. **9** (Plenum Press, New York) 1990, pp. 1669-1676.
- [5] ZHENG Y., MAEV R. GR. and SOLODOV I. YU., *Can. J. Phys.*, **77** (1999) 927.
- [6] HAMILTON M. F., IL'INSKII YU. A. and ZABOLOSTKAYA E. A., in *Nonlinear Acoustics*, edited by HAMILTON M. F. and BLACKSTOCK D. T. (Academic Press, San Diego) 1997, pp. 151-175.
- [7] MAYER A. P., *Phys. Rep.*, **256** (1995) 237.
- [8] LEAN E. G. and POWELL C. G., *Appl. Phys. Lett.*, **19** (1971) 356.
- [9] LEE J., SINGH M. P. and ZUCKER J., *Appl. Phys. Lett.*, **36** (1980) 896.
- [10] BELYAeva I. YU., OSTROVSKY L. A. and TIMANIN E. M., *Acoust. Lett.*, **15** (1992) 221.
- [11] TOURNAT V. *et al.*, *Phys. Rev. Lett.*, **92** (2004) 085502.
- [12] BELYAeva I. YU., ZAITSEV V. YU. and TIMANIN E. M., *Acoust. Phys.*, **40** (1994) 893.
- [13] ZAITSEV V. YU., *Acoust. Phys.*, **41** (1995) 439.
- [14] SILBERT L. E., GREST G. S. and LANDRY J. W., *Phys. Rev. E*, **66** (2002) 061303.
- [15] LUDING S., *Phys. Rev. E*, **55** (1997) 4720.
- [16] RADJAI F., JEAN M., MOREAU J.-J. and ROUX S., *Phys. Rev. Lett.*, **77** (1996) 274.
- [17] LIU C.-H. *et al.*, *Science*, **269** (1995) 513.